Korean Journal of Radiology

KJR

Check for updates

A Novel Melanin-Targeted ^{18}F-PFPN Positron Emission Tomography Imaging for Diagnosing Ocular and Orbital Melanoma

Yiyan Wang^{1}*, Xinghua Wang^{1}*, Jie Zhang^{1}, Xiao Zhang^{2}, Yang Cheng^{1}, Fagang Jiang^{1}

^{1}Department of Ophthalmology, Union Hospital, Tongji Medical College, Huazhong University of Science and Technology, Wuhan, China
^{2}Department of Nuclear Medicine, Union Hospital, Tongji Medical College, Huazhong University of Science and Technology, Wuhan, China

Objective: ^{18}F-N-(2-(Diethylamino)ethyl)-5-(2-(2-(2-fluoroethoxy)ethoxy)ethoxy) picolinamide (^{18}F-PFPN) is a novel positron emission tomography (PET) probe designed to specifically targets melanin. This study aimed to evaluate the diagnostic feasibility of ^{18}F-PFPN in patients with ocular or orbital melanoma.
Materials and Methods: Three patients with pathologically confirmed ocular or orbital melanoma (one male, two females; age 41–59 years) were retrospectively reviewed. Each patient underwent comprehensive ^{18}F-PFPN and ^{18}F-fluorodeoxyglucose (^{18}F-FDG) PET scans. The maximum standardized uptake value (SUV$_{max}$) of the lesion and the interference caused by background tissue were compared between ^{18}F-PFPN and ^{18}F-FDG PET imaging. In addition, the effect of intrinsic pigments in the uvea and retina on the interpretation of the results was examined. The contralateral non-tumorous eye of each patient served as a control.
Results: All primary tumors (3/3) were detected using ^{18}F-PFPN PET, while only two primary tumors were detected using ^{18}F-FDG PET. Within each lesion, the SUV$_{max}$ of ^{18}F-PFPN was 2.6 to 8.3 times higher than that of ^{18}F-FDG. Regarding the quality of PET imaging, the physiological uptake of ^{18}F-FDG PET in the brain and periocular tissues limited the imaging of tumors. However, ^{18}F-PFPN PET minimized this interference. Notably, intrinsic pigments in the uvea and retina did not cause abnormal concentrations of ^{18}F-PFPN, as no anomalous uptake of ^{18}F-PFPN was detected in the healthy contralateral eyes.
Conclusion: Compared to ^{18}F-FDG, ^{18}F-PFPN demonstrated higher detection rates for ocular and orbital melanomas with minimal interference from surrounding tissues. This suggests that ^{18}F-PFPN could be a promising clinical diagnostic tool for distinguishing malignant melanoma from benign pigmentation in ocular and orbital melanomas.
Keywords: Ocular melanoma; Orbital melanoma; Positron emission tomography; ^{18}F-FDG; ^{18}F-PFPN

INTRODUCTION

Melanoma is a malignant neoplasm originating from melanocytes and has a high mortality rate [1]. Ocular and orbital melanomas, the second most common type of melanoma following cutaneous melanomas [2], can be less intuitive to identify because they are often located within or behind the eyeball. Traditional imaging modalities, including computed tomography (CT), magnetic resonance imaging (MRI), ultrasound (US), and certain ocular examinations, such as fundus photography, fundus angiography, and optical coherence tomography, have been utilized to detect these tumors [3,4]. However, these methods have limitations. Not all tumors are easily visible in these images, as some small

ocular melanomas and ocular nevi often appear similarly [5]. Furthermore, site-specific imaging does not provide comprehensive views of the entire body.

Positron emission tomography (PET) using ^{18}F-fluorodeoxyglucose (^{18}F-FDG) is the predominant whole-body imaging modality [6]. In clinical practice, ^{18}F-FDG PET has proven useful for identifying [7,8], staging [9], and predicting the prognosis [10] of patients with advanced (stage III-IV) or medium-to-large uveal melanomas (UMs). However, it has insufficient sensitivity for detecting stages I–II and small UMs [8]. Additionally, ^{18}F-FDG PET imaging may be limited by uptake in periocular tissues, such as the brain [11], which can affect the detection of ocular and orbital tumors.

[18]F-N-(2-(Diethylamino)ethyl)-5-(2-(2-(2-fluoroethoxy) ethoxy)ethoxy) picolinamide (^{18}F-PFPN) is an emerging melanin-specific PET tracer targets melanin in tumors [12]. Given that over 90% of melanomas contain melanin [13], the potential applications of ^{18}F-PFPN are substantial. Recent studies have highlighted the safety and tolerability of ^{18}F-PFPN in humans [14]. Compared to ^{18}F-FDG, ^{18}F-PFPN demonstrated higher detection rates in skin and rectal melanomas and could pinpoint metastatic lesions smaller than 2 mm [14]. To date, there have been no systematic studies on ^{18}F-PFPN in ocular and orbital melanomas. This study aimed to investigate the diagnostic feasibility of ^{18}F-PFPN in patients with ocular or orbital melanoma and to examine the effect of intrinsic pigments in the uvea and retina on ^{18}F-PFPN imaging in the contralateral healthy eyes of these patients.

MATERIALS AND METHODS

Patients

This retrospective analysis included selected patients from a trial (ClinicalTrials.gov number: NCT04747561) approved by the local Institutional Ethics Committee (IRB No. 2021-0016). All the participants provided written informed consent. From August 2022 to September 2023, three patients (one male and two females; age 41–59 years) with pathologically confirmed ocular or orbital melanoma at our hospital were retrospectively analyzed. Demographic data, clinical presentation, tumor location, and size, ^{18}F-PFPN and ^{18}F-FDG PET results, and other imaging findings, including CT, MRI, US, fundus photography, and fundus fluorescein angiography, were collected.

Image Acquisition

The patients underwent both ^{18}F-PFPN PET/MRI and ^{18}F-FDG PET/CT imaging sessions within a brief interval (no more than one week) of each other. All scans covered the entire body, from the brain to the foot.

^{18}F-PFPN PET/MR Imaging

^{18}F-PFPN, a molecular probe that specifically binds to melanin, was synthesized as described previously [12]. ^{18}F-PFPN PET/MRI was performed using a Signa PET/MR scanner (SIGNA[TM] PET/MR; GE Healthcare, Chicago, IL, USA). Each patient received an intravenous injection of ^{18}F-PFPN at a dose of 3.0–5.4 MBq/kg, followed by whole-body PET/MR imaging after a two-hour rest period. Axial T1-weighted MR was performed using the LAVA-FLEX sequence, while coronal T2-weighted MR was performed using the fast-recovery fast spin-echo sequence. PET image reconstruction utilizes the ordered subset maximization iterative method with a combined time-of-flight technique and a point diffusion function comprising two iterations and 28 subsets, followed by Gaussian filtering (3 mm) for image processing.

^{18}F-FDG PET/CT Imaging

PET/CT imaging was conducted using a PET/CT scanner (Discovery VCT®; GE Healthcare, Milwaukee, WI, USA). Patients underwent a minimum six-hour fasting period, and ^{18}F-FDG was administered intravenously at a dose of 3.7–5.4 MBq/kg after ensuring that their blood glucose was below 11.1 mmol/L. Subsequently, PET/CT imaging was performed after sixty minutes of calm rest. CT images were obtained with parameters set at 120 kV, 80 mA, and a thickness layer of 3.75 mm. PET image reconstruction was performed using the ordered subset expectation maximization iterative method with a reconstruction matrix of 512 x 512 and a thickness of 3 mm.

Image Interpretation

The lesion volumes of interest were mapped on PET/MRI and PET/CT fusion images using the three-dimensional outlining method on the Advantage Workstation version AW4.6 (GE Healthcare, Milwaukee, WI, USA). The system automatically calculated the maximum standardized uptake value (SUV_{max}) of the lesions. The raw SUV_{max} was normalized using the method described by Zhang et al. [14].

$$Normalized\ SUV_{max} = raw\ SUV_{max}/SUV_{bkgd}$$

Where SUV_{bkgd} refers to the mean SUV_{max} of the descending aorta.

The SUV_{max} of ^{18}F-PFPN and ^{18}F-FDG within lesions was quantitatively compared, using pathological findings as the basis for the final diagnosis. Additionally, the effect of intrinsic pigments in the uvea and retina on the interpretation of the results was examined, with the contralateral non-tumorous eye of each patient serving as a control.

RESULTS

This study evaluated three patients who underwent multimodal imaging. The clinical manifestations and imaging findings of each patient are shown in Table 1. The participants included three types of patients with melanomas occurring in different anatomical locations of the eye. Patient #1 was a 59-year-old female with melanoma of the eyelid and conjunctiva (Supplementary Fig. 1); patient #2 was a 49-year-old female with orbital melanoma (Supplementary Fig. 2); and patient #3 was a 41-year-old male with choroidal melanoma (Supplementary Fig. 3).

Our results showed that ^{18}F-PFPN had a higher detection rate than ^{18}F-FDG in these melanomas. This enhanced performance is evident from two primary observations.

Firstly, abnormal accumulation of ^{18}F-PFPN was evident in the primary tumors of all participants (3/3). In contrast, only two participants (2/3) showed high uptake levels using ^{18}F-FDG (patient #1: Fig. 1, patient #2: Fig. 2, patient #3: Fig. 3). One tumor lesion was missed when using ^{18}F-FDG, likely because of the small size of the tumor. Secondly, the SUV_{max} of ^{18}F-PFPN consistently exceeded that of ^{18}F-FDG within the same patient, ranging from 2.6 to 8.3 times greater.

Subsequently, we compared the imaging quality of ^{18}F-PFPN and ^{18}F-FDG PET scans. The results showed that ^{18}F-PFPN PET provided a clearer visualization of lesions owing to the low background uptake. In contrast, ^{18}F-FDG PET images showed interference in the visualization of ocular and orbital melanomas because of physiological uptake in the brain and periocular tissues (Figs. 1B, 2B, 3B: green boxes). This interference was reduced in ^{18}F-PFPN PET images (Figs. 1A, 2A, 3A: red boxes). Moreover, neither ^{18}F-PFPN nor ^{18}F-FDG scans showed abnormal concentrations in the contralateral non-tumor eye of any participant, which is in line with the self-referential comparison.

No metastases were detected in any patient. Patient #2 underwent excision of an intraorbital mass; however, follow-up scans using both ^{18}F-FDG and ^{18}F-PFPN PET revealed tumor residue in the orbital cavity.

Table 1. Clinical presentations and imaging findings of patients with ocular and orbital melanoma

	Patient #1	Patient #2	Patient #3
Sex	Female	Female	Male
Age, yr	59	49	41
Clinical features	Pigmented mass in the right eye	Swelling in the right eye	A dark shadow covered the right eye
Tumor			
Location	Eyelid and conjunctiva	Orbit	Choroid
Size, mm	13 x 5 x 5	33 x 27	11 x 6
SUV_{max} of the primary tumor			
^{18}F-PFPN	16.6	36.2	10.6
^{18}F-FDG	2.0	9.2	4.1
^{18}F-PFPN:^{18}F-FDG	8.3:1.0	3.9:1.0	2.6:1.0
Other imaging methods and findings			
MR*	High T1WI and high T2WI	High T1WI and low T2WI	High T1WI and low T2WI
CT	Nodular enhancement signal	Nodular mixed signal	High-density signal with significant enhancement
US	-	-	Dome-shaped mass
FP	-	-	Caesious local solid bulge
FFA	-	-	Punctate hyper fluorescence in filling phases

*MR protocols: axial T1-weighted MR was conducted using the LAVA-FLEX sequence, and coronal T2-weighted MR was performed using the fast-recovery fast spin-echo sequence.

MR = magnetic resonance, SUV_{max} = maximum standardized uptake value, ^{18}F-PFPN = ^{18}F-N-(2-(Diethylamino)ethyl)-5-(2-(2-(2-fluoroethoxy)ethoxy)ethoxy)picolinamide, ^{18}F-FDG = ^{18}F-fluorodeoxyglucose, T1WI = T1-weighted image, T2WI = T2-weighted image, CT = computed tomography, US = ultrasound, FP = fundus photography, FFA = fundus fluorescein angiography
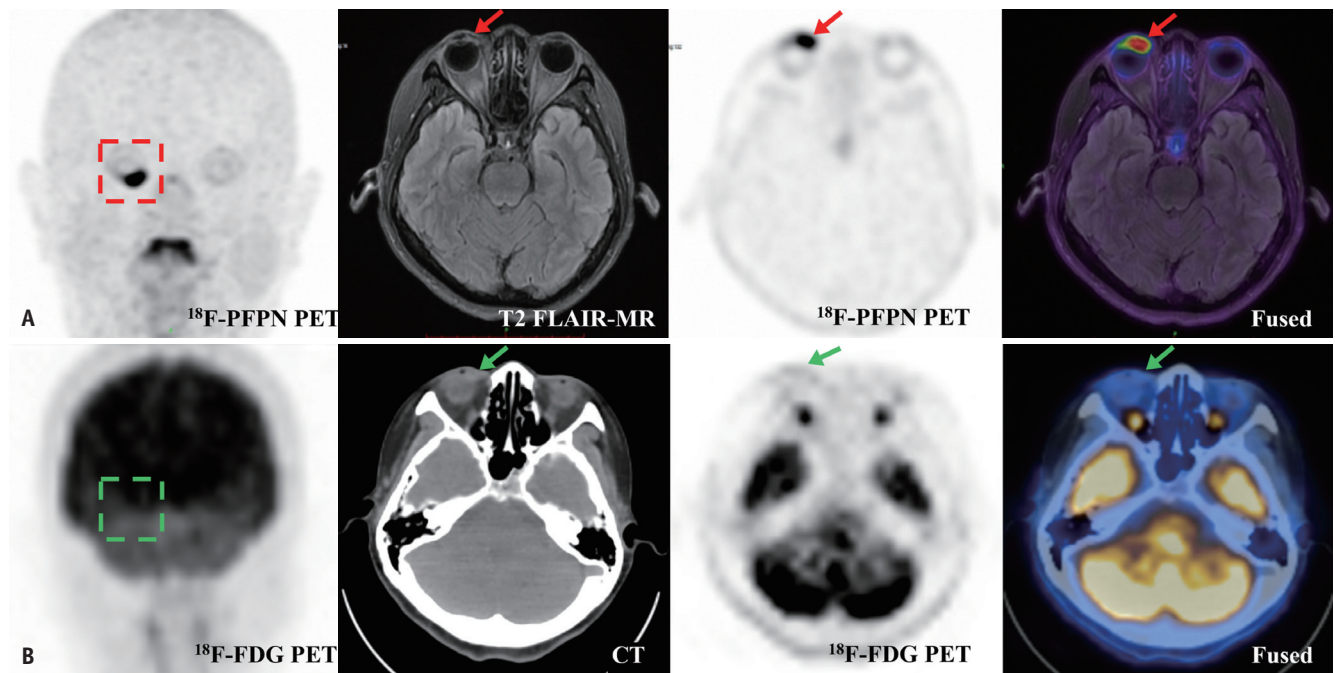
Fig. 1. A 59-year-old female with melanoma of the eyelid and conjunctiva. **A:** In ^{18}F-PFPN PET images, the tumor lesion (red box and arrows) can be clearly visualized. The SUV$_{max}$ of ^{18}F-PFPN at the lesion was 16.6. MR imaging demonstrated an abnormal signal shadow in the lower lid of the right eye. **B:** In ^{18}F-FDG PET images, the brain and periocular tissues interfered with the visualization of the tumor, which made it difficult to identify the tumor (green box and arrows). The SUV$_{max}$ of ^{18}F-FDG at the lesion was 2.0. A thickened lesion site could be seen in the CT image. ^{18}F-PFPN = ^{18}F-N-(2-(Diethylamino)ethyl)-5-(2-(2-(2-fluoroethoxy)ethoxy)ethoxy) picolinamide, PET = positron emission tomography, SUV$_{max}$ = maximum standardized uptake value, MR = magnetic resonance, ^{18}F-FDG = ^{18}F-fluorodeoxyglucose, CT = computed tomography, FLAIR = fluid-attenuated inversion recovery

DISCUSSION

This study describes the clinical presentations and imaging characteristics of a cohort of patients diagnosed with ocular or orbital melanomas. Furthermore, we compared the diagnostic efficacy of ^{18}F-PFPN with ^{18}F-FDG in these tumors. We preferred to combine MR with PET, especially when using ^{18}F-PFPN as a tracer because the inherent paramagnetic properties of pigmented lesions can be observed on MR. These lesions often exhibit characteristic high signals on T1-weighted images and low signals on T2-weighted images, which can enhance the accuracy of image analysis.

This study found that ^{18}F-PFPN showed higher detection rates for ocular and orbital melanomas than ^{18}F-FDG, and had less interference from background tissues. This finding is similar to that of Zhang et al. [14], who reported that ^{18}F-PFPN could detect T2b stage melanoma and that the SUV$_{max}$ of ^{18}F-PFPN at the primary site was 3.92 times higher than that of ^{18}F-FDG. Although none of the patients in this study had metastases, Zhang et al. [14] showed that ^{18}F-PFPN could detect more and smaller melanoma metastases, identifying 365 metastases that were missed by

^{18}F-FDG, including one smaller than 2 mm.

Although ^{18}F-PFPN targets melanin, the normal presence of pigments in the retinal and uveal tissues does not appear to interfere with the results of ^{18}F-PFPN. In this study, no abnormal concentrations of ^{18}F-PFPN were detected in the contralateral normal eyes of any patient. In a study of a healthy population, the mean SUV in eye tissue increased from 0.79 ± 0.07 at 30 minutes after injecting ^{18}F-PFPN to 1.32 ± 0.30 at 240 minutes, but these levels did not meet the criteria for pathological evaluation [14]. This finding suggests that ^{18}F-PFPN has the potential to distinguish malignant melanomas from benign pigmentation.

Although ^{18}F-PFPN has shown many advantages in detecting melanoma, it may not be as sensitive as ^{18}F-FDG for identifying amelanotic melanoma [12,14], which accounts for approximately 2%–8% of melanomas [15]. This study presents a novel diagnostic challenge. This study has some limitations. First, the relative scarcity of these cases led to a limited sample size, preventing a more detailed statistical analysis of the data. Second, patients with nevi or other pigmented diseases requiring differentiation from malignant melanoma were not included. This will be the
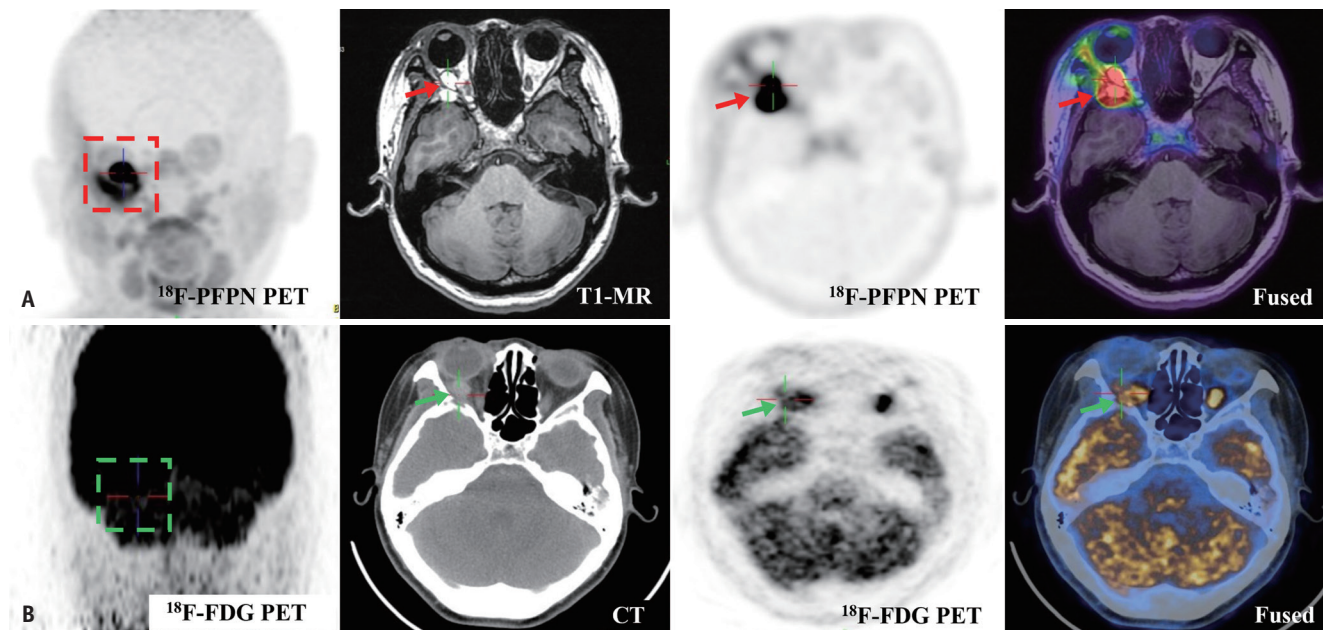
Fig. 2. A 49-year-old female with orbital melanoma. **A:** In ^{18}F-PFPN PET images, showing the upper portion of the lesion and its relationship to the ocular structures (the entire extent of the lesion is presented in Supplementary Fig. 2), the tumor lesion (red box and arrows) can be clearly visualized. The SUV$_{max}$ of ^{18}F-PFPN at the lesion was up to 36.2. MR imaging demonstrated an occupation within the right orbit with a high signal on T1-weighted images and a low signal on T2-weighted images. The occupation pushed against the rectus externus, rectus internus, and optic nerve, and breached the adjacent great wing of the sphenoid bone. **B:** In ^{18}F-FDG PET images, the brain and periocular tissues interfered with the visualization of the tumor, which made it difficult to identify the tumor (green box and arrows). The SUV$_{max}$ of ^{18}F-FDG at the lesion was 9.2. CT demonstrated an abnormal soft tissue density shadow within the right orbit. ^{18}F-PFPN = ^{18}F-N-(2-(Diethylamino)ethyl)-5-(2-(2-(2-fluoroethoxy)ethoxy)ethoxy) picolinamide, PET = positron emission tomography, SUV$_{max}$ = maximum standardized uptake value, MR = magnetic resonance, ^{18}F-FDG = ^{18}F-fluorodeoxyglucose, CT = computed tomography

focus of future studies.

To the best of our knowledge, this is the first study to evaluate the ability of melanin-targeted ^{18}F-PFPN to detect ocular and orbital melanomas. Compared to ^{18}F-FDG, ^{18}F-PFPN demonstrated higher detection rates for ocular and orbital melanomas and experienced minimal interference from the surrounding tissues. This suggests that ^{18}F-PFPN may be a promising clinical diagnostic tool for ocular and orbital melanomas, with the potential to distinguish malignant melanomas from benign pigmentation. Future research should aim to verify these results with a larger sample size and explore the potential of ^{18}F-PFPN to differentiate other pigmentary lesions and their use in adjuvant therapy options.

Supplement

The Supplement is available with this article at https://doi.org/10.3348/kjr.2024.0243.

Availability of Data and Material
The datasets generated or analyzed during the study are

available from the corresponding author on reasonable request.

ORCID IDs
Yiyan Wang
    https://orcid.org/0009-0003-9551-023X
Xinghua Wang
    https://orcid.org/0000-0002-5608-0607
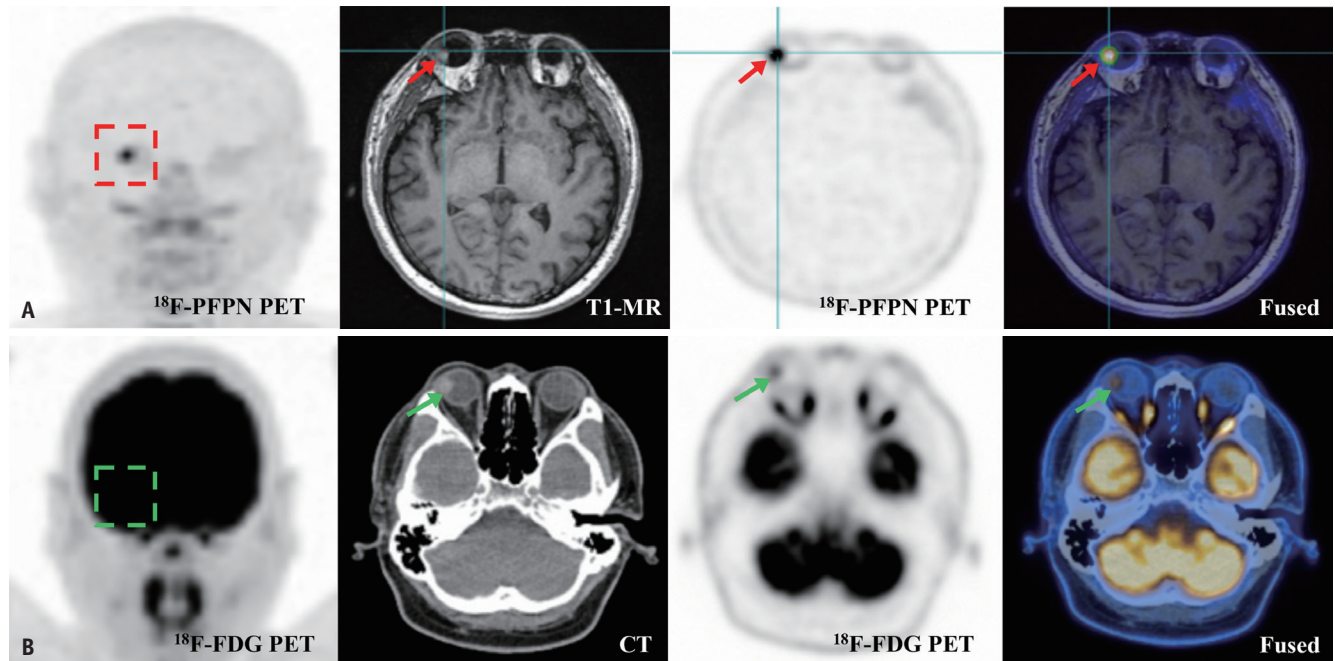
Fig. 3. A 41-year-old male with choroidal melanoma. **A:** In ^{18}F-PFPN PET images, the tumor lesion (red box and arrows) can be clearly visualized. The SUV$_{max}$ of ^{18}F-PFPN at the lesion was 10.6. MR imaging demonstrated an abnormal signal shadow in the lateral wall within the right eyeball, with a high signal on T1-weighted images and a low signal on T2-weighted images. **B:** In ^{18}F-FDG PET images, the brain and periocular tissues interfered with the visualization of the tumor, which made it difficult to identify the tumor (green box and arrows). The SUV$_{max}$ of ^{18}F-FDG at the lesion was 4.1. CT demonstrated an abnormal density shadow in the lateral wall within the right eyeball. ^{18}F-PFPN = ^{18}F-N-(2-(Diethylamino)ethyl)-5-(2-(2-(2-fluoroethoxy)ethoxy)ethoxy) picolinamide, PET = positron emission tomography, SUV$_{max}$ = maximum standardized uptake value, MR = magnetic resonance, ^{18}F-FDG = ^{18}F-fluorodeoxyglucose, CT = computed tomography

Jie Zhang
  https://orcid.org/0000-0003-2754-9629
Xiao Zhang
  https://orcid.org/0000-0002-7305-5278
Yang Cheng
  https://orcid.org/0009-0006-1778-0797
Fagang Jiang
  https://orcid.org/0009-0005-7715-4993

REFERENCES

1. Arnold M, Singh D, Laversanne M, Vignat J, Vaccarella S, Meheus F, et al. Global burden of cutaneous melanoma in 2020 and projections to 2040. *JAMA Dermatol* 2022;158:495-503
2. McLaughlin CC, Wu XC, Jemal A, Martin HJ, Roche LM, Chen VW. Incidence of noncutaneous melanomas in the U.S. *Cancer* 2005;103:1000-1007
3. Verbeek S, Dalvin LA. Advances in multimodal imaging for diagnosis of pigmented ocular fundus lesions. *Can J Ophthalmol* 2023 Jul 19 [Epub]. https://doi.org/10.1016/j.jcjo.2023.07.005
4. Foti PV, Travali M, Farina R, Palmucci S, Spatola C, Raffaele L, et al. Diagnostic methods and therapeutic options of uveal melanoma with emphasis on MR imaging-Part I: MR imaging with pathologic correlation and technical considerations. *Insights Imaging* 2021;12:66
5. Singh AD, Raval V, Wrenn J, Zabor EC. Small choroidal melanoma: outcomes after surveillance versus immediate treatment. *Am J Ophthalmol* 2022;241:47-56
6. Schwenck J, Sonanini D, Cotton JM, Rammensee HG, la Fougère C, Zender L, et al. Advances in PET imaging of cancer. *Nat Rev Cancer* 2023;23:474-490
7. Papastefanou VP, Islam S, Szyszko T, Grantham M, Sagoo MS, Cohen VM. Metabolic activity of primary uveal melanoma on PET/CT scan and its relationship with monosomy 3 and other prognostic factors. *Br J Ophthalmol* 2014;98:1659-1665
8. Reddy S, Kurli M, Tena LB, Finger PT. PET/CT imaging: detection of choroidal melanoma. *Br J Ophthalmol* 2005;89:1265-1269
9. Freton A, Chin KJ, Raut R, Tena LB, Kivelä T, Finger PT. Initial PET/CT staging for choroidal melanoma: AJCC correlation and second nonocular primaries in 333 patients. *Eur J Ophthalmol* 2012;22:236-243
10. Lee CS, Cho A, Lee KS, Lee SC. Association of high metabolic activity measured by positron emission tomography imaging

with poor prognosis of choroidal melanoma. *Br J Ophthalmol* 2011;95:1588-1591

11. Stelter L, Evans MJ, Jungbluth AA, Zanzonico P, Ritter G, Ku T, et al. Novel mechanistic insights into arginine deiminase pharmacology suggest 18F-FDG is not suitable to evaluate clinical response in melanoma. *J Nucl Med* 2012;53:281-286

12. Xu X, Yuan L, Yin L, Jiang Y, Gai Y, Liu Q, et al. Synthesis and preclinical evaluation of 18F-PEG3-FPN for the detection of metastatic pigmented melanoma. *Mol Pharm* 2017;14:3896-3905

13. Rouanet J, Quintana M, Auzeloux P, Cachin F, Degoul F. Benzamide derivative radiotracers targeting melanin for melanoma imaging and therapy: preclinical/clinical development and combination with other treatments. *Pharmacol Ther* 2021;224:107829

14. Zhang X, Li M, Gai Y, Chen J, Tao J, Yang L, et al. 18F-PFPN PET: a new and attractive imaging modality for patients with malignant melanoma. *J Nucl Med* 2022;63:1537-1543

15. Thomas NE, Kricker A, Waxweiler WT, Dillon PM, Busman KJ, From L, et al. Comparison of clinicopathologic features and survival of histopathologically amelanotic and pigmented melanomas: a population-based study. *JAMA Dermatol* 2014;150:1306-1314